

LAMB WAVE ANALYSIS AND DAMAGE DETECTION IN A SKIN-STRINGER COMPOSITE JOINT

LENKA ŠEDKOVÁ^{*}, ONDŘEJ VÍCH^{*} AND JAKUB ŠEDEK^{*}

^{*} Czech Aerospace Research Centre (VZLU)
Aviation division
Beranovych 130, 19905 Prague
e-mail: sedkova@vzlu.cz, web page: <http://www.vzlu.cz>

Key words: Lamb waves, Skin-stringer joint, Thermoplastic composites, Impact damage detection, Probabilistic algorithm.

Abstract. *Lamb wave qualitative analysis and impact damage detection in a bolted skin-stringer thermoplastic composite component were performed. The structure belongs to an aircraft structural part and represents a complicated structure from the Lamb wave mode identification perspective, especially when the joint is realized only by Hi-Lok fasteners. The sensor network for damage detection included 16 PZT disc transducers, however, additional sensors were exploited for supporting measurements. Two frequencies, representing A0 and S0 modes, were used to evaluate the propagation across the joint. Several impact damages were introduced to the stringer and skin parts of the structure. Suitable propagation mode and frequency for damage detection within the specific skin-stringer part were identified. Sensor configuration divided the test specimen into several sections and enabled measurements within a specific section with a specific frequency. The time delay of A0 mode at 50 kHz was exploited for impact damage detection within the skin part, and S0 mode at 180 kHz within the stringer part. The probabilistic algorithm was successfully used for the damage imaging. The damage index was based on the time delay of the selected mode, comparing baseline measurement and measurement in the damaged state. This study provides a possible methodology for structural health monitoring of aircraft structural parts made from bolted thermoplastic composite skin-stringer joints.*

1 INTRODUCTION

Composite skin-stringer assemblies are often used as principal structural elements in aircraft wings or fuselage. The stringer part stiffens the skin and the whole assembly may be designed in various ways. Mostly there is a joint between the skin and the stringer, either an adhesively bonded composite joint, bolted joint, or both, or the assembly may be designed even as an integral part [1]. In the case of the damage tolerance philosophy, the integrity of the structure during the operation needs to be assured by regular NDI (Non-destructive Inspection) or by the

SHM (Structural Health Monitoring) tools. The inspection/monitoring strategy is based on the possible flaws that may occur within the given structure. Generally, the structure may be sensitive to impact damages, the adhesively bonded joint may be prone to debonding and a combination of loads and impacts may cause critical failure.

Monitoring using ultrasonic guided waves, specifically Lamb waves, is one of the leading SHM methods for plate-like aircraft structures [2]. Many papers have been published regarding Lamb-wave-based damage detection of aircraft composite structures. Regarding impact damage detection numerical analyses and experimental tests on different levels of the building block approach have been conducted. Even large composite panels representing aircraft fuselage have been tested with the output of probability of detection (POD) curves [3,4]. In publication [5] it was found that quasi-isotropic stiffness constants are degraded in the impact-damaged region leading to the time delay of A0 due to change in C_{33} . The time delay of A0 mode as an impact damage-sensitive parameter has been used also in our previous publications [6, 7]. The signal magnitude change or time reversal approach was exploited for barely visible impact damage in [8]. Damage-sensitive parameters can be processed in various ways. Imaging algorithms such as the reconstruction algorithm for the probabilistic inspection of damage (RAPID) are very popular. RAPID is described e.g. in [9, 10], and enables to use a variety of signal parameters as damage indices (DIs) [4]. The influence of the algorithm parameters affecting the damage identification is analyzed in [11].

In this paper, a thermoplastic composite skin-stringer joint is realized by Hi-Lok fasteners without any adhesive, therefore, the structure is subjected to impact damages in different parts of the assembly. The strategy for Lamb wave actuation, detection, and evaluation is introduced. Preliminary measurements focused especially on qualitative measurements. Utilization of the first detected wavepacket is essential for evaluation. Therefore, additional sensors were placed on the structure to identify propagating modes towards the skin and the stringer. This information was exploited together with dispersion curves to the suitable frequency selection. Finally, impact damages were realized and evaluated using the RAPID.

2 TEST SPECIMEN

Two test specimens designated as Omega 1 and Omega 2 were manufactured from carbon composite with PPS (polyphenylene sulphid) thermoplastic matrix. The skin-stringer joints were realized only by Hi-Loks, without any adhesive. The structural design needs to be taken into account regarding the sensor network layout, Lamb wave actuation parameters, and damage detection strategy.

Sixteen PZT disc sensors (No. 1-16) by StemInc were mounted on the test specimens dividing the assembly into four subsections, according to Figure 1a. These sensors were used for damage detection. Sensors No. 23-32 were mounted additionally along the cross-section (Figure 1b) to evaluate Lamb wave propagation qualitatively.

Acclent Scan Genie II was used as a data acquisition unit. Origin Pro SW and in-house RAPID algorithm tool were utilized for data postprocessing.

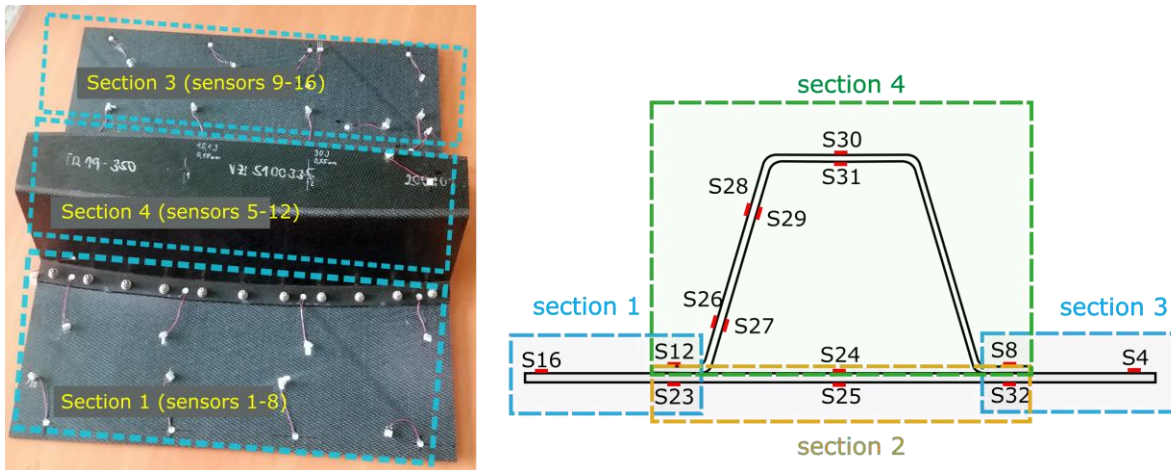


Figure 1: Omega test specimen a) image, b) cross-section scheme

3 PRELIMINARY MEASUREMENTS

3.1 Dispersion curves

Segments of phase velocity dispersion curves were determined experimentally using the FFT (Fast Fourier transform) filtering method [12] and compared to the calculations using the GUIGUW SW [13]. GUIGUW is based on the SAFE (Semi-analytical finite element) method [9]. Material parameters were used the same as for the plates analyzed in the publication [12]. The skin-stringer assembly is manufactured from the same material.

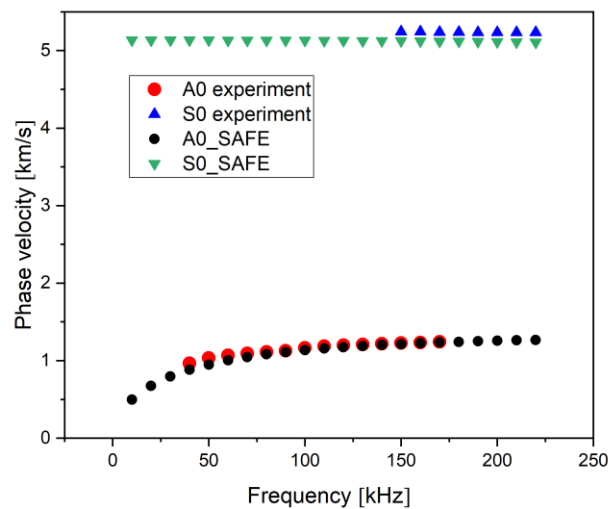


Figure 2: A segment of a phase velocity dispersion curve – experimental and calculated values

3.2 Qualitative evaluation of Lamb wave propagation

Skin-stringer joint represents a complicated structure from the perspective of mode identification. Unlike the propagation in a simple plate, the joint may cause mode conversion. Together with multiple reflections, mode identification is difficult without numerical simulations or experimental methods of full wavefield imaging. Due to the lack of these techniques, supporting measurements were also performed. Additional sensors (No. 23-32) were mounted on the test specimens, according to Figure 1b. Sensors were placed symmetrically along the cross-section line on both surfaces. This placement allows mode determination. Out-of-phase signals indicate asymmetrical mode and in-phase signals symmetrical mode. The aim was to assess Lamb wave behavior on the joint and determine frequencies at which the specific modes propagate into the skin and the stringer as the first detected wave packets.

Signals were actuated from the joint at both surfaces (S12/S23). Wave propagation through the joint and the subsequent propagation to the stringer and/or to the skin, and finally to the joint on the other side was observed. The examples of some wave packets are shown in Figure 3 for the frequencies of 50 kHz and 180 kHz, representing A0 and S0 modes, respectively. Other waveforms detected along the whole cross-section are published in [13]. Figure 3a shows the signal actuated at the upper side of the first joint (S12) and detected at the second joint (S8 and S32). At the frequency of 50 kHz, the signals are out-of-phase, hence the propagating mode is A0. Based on the velocity dispersion curves and other waveforms along the cross-section of the stringer and the skin, the first detected wavepacket propagated along the skin (shorter distance) and the other wavepacket along the stringer. The attenuation by the joint is not significant for A0 mode. The same situation for the frequency of 180 kHz is presented in Figure 3b. S0 mode propagates along the stringer with significant attenuation at the joint. Therefore, there is a very low-amplitude signal detected at the bottom side of the joint (S32), and no wavepacket was determined as a wavepacket propagated along the skin. A completely different situation is when actuating at the bottom side of the joint (S23) – see Figure 3c. The wave S0 does not penetrate through the joint to the stringer and propagates only along the skin. The first detected wavepacket is identified as S0 mode and the third as A0 mode. This signal shows that S0 is much more attenuated by the joint than A0 mode.

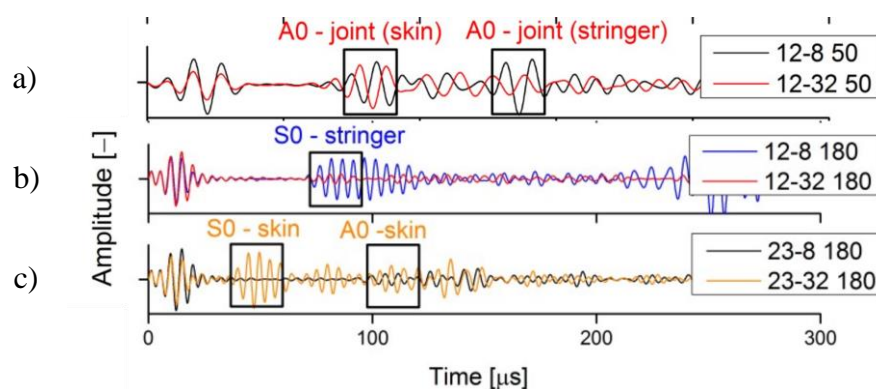


Figure 3: Wave propagation actuated from the area of the joint at the frequency of a) 50 kHz and b, c) 180 kHz

3.3 Monitoring strategy

Sixteen PZT sensors were divided into four groups monitoring those four subsections of the test assembly. Each subsection was monitored using 8 PZTs. Sensors within sections 1 (No. 1-8), 2 (No. 5-12), and 3 (9-16) covered the skin, and section 4 (No. 5-12) covered the stringer. Sensors No. 5-12 mounted on the joint covered both, the skin part and the stringer part. However, based on the previous analysis, S0 mode at the frequency of 180 kHz was used for the stringer monitoring and A0 mode at 50 kHz for the skin monitoring.

The reasons are as follows:

1. Section 4 – the stringer part: S0 mode at the frequency of 180 kHz does not propagate dominantly into the skin due to the presence of the joint. Therefore, the first detected wave packet was identified as the wave packet propagated through the stringer.
2. Section 1, 2, 3: A0 mode at the frequency of 50 kHz propagates along all the skin parts as the first identified wavepacket. Based on previous measurements on plates A0 mode at lower frequency is more sensitive to impact damage [13].

RAPID algorithm was used for damage detection and visualization. The damage index (DI) was based on the time delay of the respective wavepacket. In case of impact damage, the time delay is caused by local stiffness degradation [5] leading to the change in the Lamb wave velocity.

4 IMPACT DAMAGE DETECTION

Seven impact damages in total were introduced to the test specimens Omega 1 and Omega 2. The locations are shown in Figure 4 and the impact boundaries are determined by means of ultrasonic A-scan. Parameters of individual impacts in terms of energy and depth are specified in Table 1. Six of them were introduced into the stringer part (section 4) and one to the skin part (section 1).

Table 1 Impact specifications

Omega 1 – Section 4			Omega 2 – Section 4		
I1*	15 J	0.18 mm	I1**	20 J	0.49 mm
I2*	30 J	0.55 mm	I2**	35 J	1.04 mm
I3**	40 J	0.99 mm	I3**	40 J	1.29 mm
Omega 1 – Section 1					
I4**	30 J	2.16 mm			

*16 mm impactor, ** 1 inch impactor

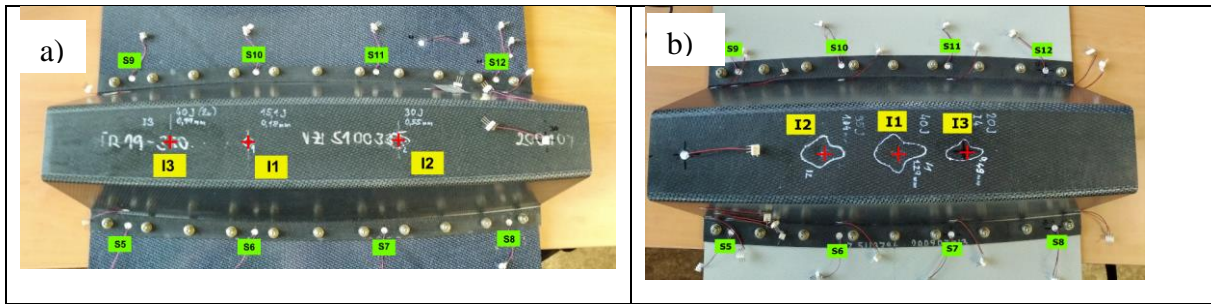


Figure 4 Test specimen a) Omega 1, b) Omega 2

The RAPID visualisation algorithm realized through in-house RAPID GUI SW was used for the damage localization in both, the skin and the omega profile. Figure 5a-c shows results for Omega 1 test specimen. Impacts I1 and partly I2 introduced with the 16 mm impactor could not be localized clearly. On the other hand, the location of I3, which was introduced by a 1-inch impactor, was detected correctly. The impact damage area of I1 is significantly smaller than the rest of them. Impact damage performed to the skin part is seen in Figure 5d.

Impact damage areas at the test specimen Omega 2 are much larger than impact damage areas at the test specimen Omega 1. Figure 6a-c shows that all impacts (I1, I2, and I3) introduced by the 1-inch impactor were localized correctly. In addition, the evaluation of two impacts at once was performed correctly (Figure 6d).

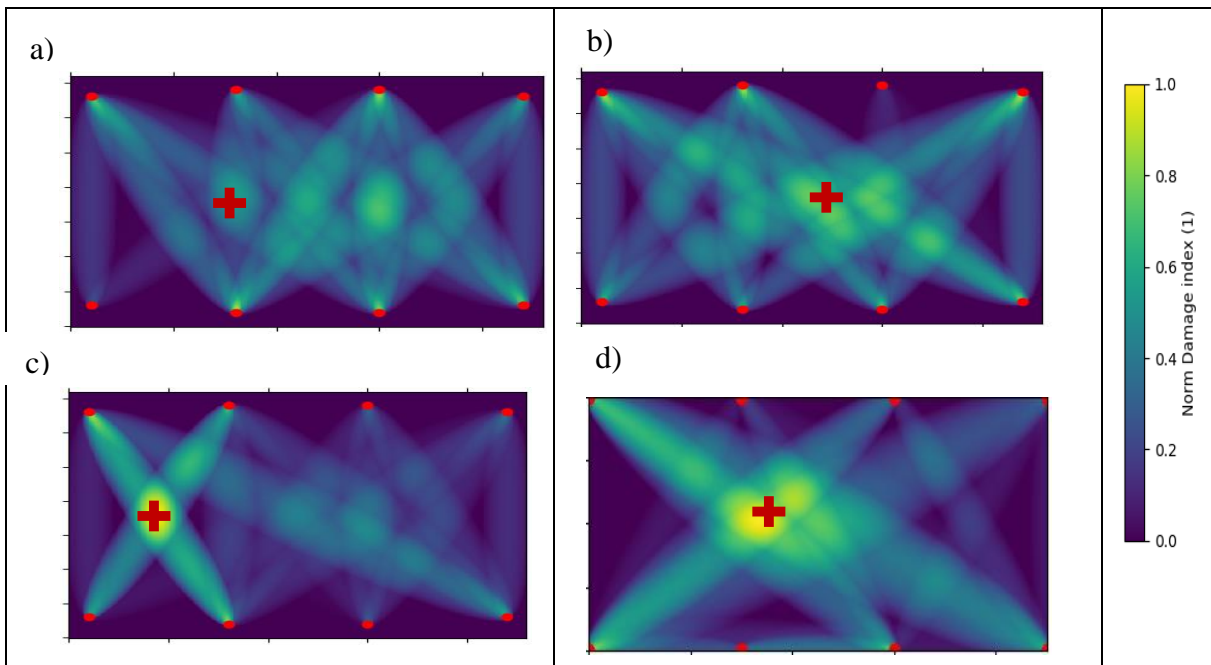


Figure 5: Omega 1 impact localization using RAPID a) I1, b) I2, c) I3, d) I4

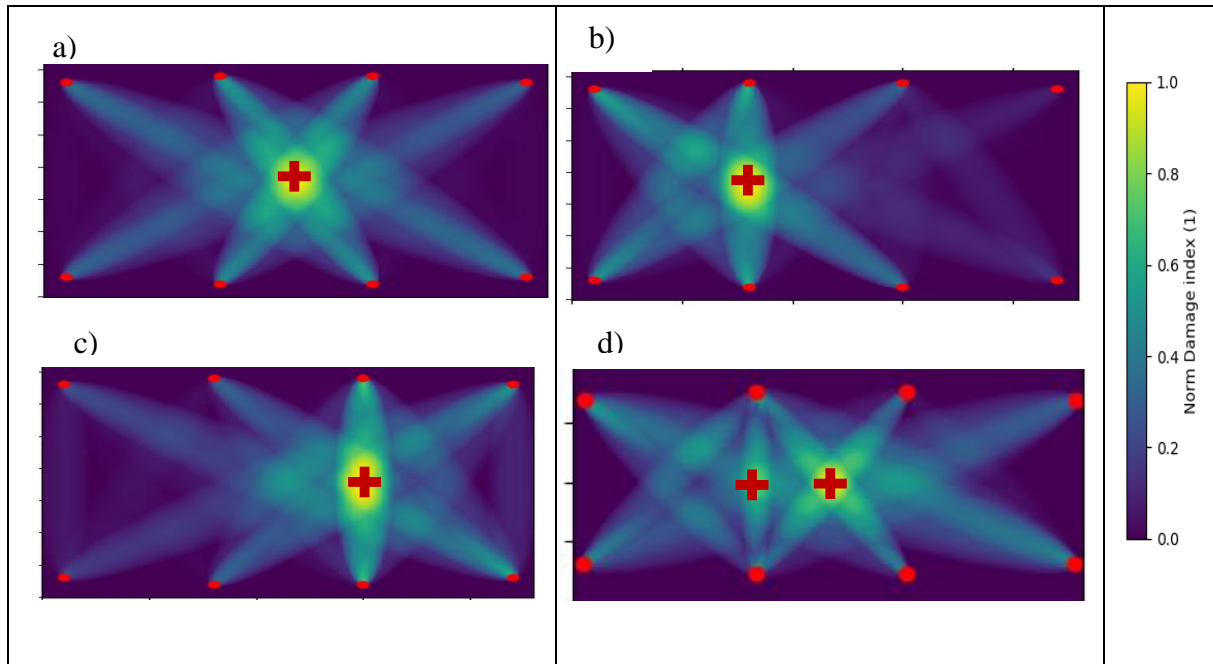


Figure 6: Omega 2 impact localization using RAPID a) I1, b) I2, c) I3, d) I1+I2

5 CONCLUSIONS

Based on the preliminary measurements at frequencies of 50 kHz and 180 kHz, the following conclusions have been drawn:

1. S0 mode is dominant at the frequency of 180 kHz
2. A0 is dominant at the frequency of 50 kHz
3. The propagation of the S0 mode at 180 kHz through the skin-stringer joint shows significant energy loss. A0 at 50 kHz does not show significant amplitude decrease.

The following conclusions have been drawn for damage monitoring:

4. Specific actuator-sensor configuration and frequency and mode selection can be exploited to ensure Lamb wave propagation only towards the stringer or towards the skin. A suitable sensor configuration for the separate monitoring of the skin and the stringer (section 2 and section 4) is at the stringer part of the joint. Sensors mounted at the joint – sensors 5-8 and 9-12 can be exploited for stringer monitoring using the S0 mode and for skin monitoring using the A0 mode.

- a. S0 mode propagation into the stringer is dominant. The frequency of 180 kHz was selected for evaluation. Propagation into the skin is eliminated by attenuation caused by the joint. S0 mode is clearly identified for all actuator-sensor paths as the first detected wave packet.
 - b. A0 mode is dominant and clearly identified at lower frequencies and is suitable for impact damage assessment within the skin part. The frequency of 50 kHz was selected for evaluation. Actuating at the stringer part of the joint, the wave propagates both into the stringer and the skin, however, due to the shorter distance, the first detected wavepackets propagated through the skin.
5. A0 mode is suitable for monitoring all the skin parts.
 6. Six impact damages were introduced into the stringer. Five of them were localized correctly. Impact damage boundaries were marked by ultrasonic A-scans. The one unidentified impact damage area was significantly smaller than the other five. The method limitation exploiting S0 mode lies probably in the damage extent.
 7. One impact damage was introduced into the skin. The impact was localized correctly using A0 mode.

The objective of this research was to develop a monitoring strategy for the skin-stringer assembly with the joint realized only by Hi-Lok fasteners. The structure was divided into four subsections and only 16 PZT sensors were exploited for monitoring. It was found out, that the stringer part and the bottom skin part are possible to be monitored using the same 8 PZT sensors mounted on the stringer part of the joint when actuating at two different frequencies.

REFERENCES

- [1] Michalcová, L., Bělský, P., Petrusová, L. Composite panel structural health monitoring and failure analysis under compression using acoustic emission. *J. Civil. Struct. Health. Monit.* (2018) **8**: 607–615.
- [2] Giurgiutiu, V., *Structural Health Monitoring of Aerospace Composites*, Academic Press, (2015).
- [3] Rodrigues, F. de Sá, Giannakeas, I. N., Khodaei, Z. Sharif, Aliabadi, F. M. H. Probability based damage detection on a composite fuselage panel based on large data set of guided wave signals. *NDT E Int.* (2023) **139**:102924
- [4] Bonet, M., Eckstein, B., Loendersloot, R., Wierach, P. Identification of Barely Visible Impact Damages on a Stiffened Composite Panel with a Probability-based Approach. *Proceedings of the European Workshop on Structural Health Monitoring*, (2015).

- [5] Deng, P., Saito, O., Okabe, Y., Soejima, H. Simplified modeling method of impact damage for numerical simulation of Lamb wave propagation in quasi-isotropic composite structures. *Compos. Struct.* (2020) **243**: 112-150.
- [6] Šedková, L., Šedek, J. Defect detectability in composite plates with variable thickness using Lamb waves. International Scientific Conference on Experimental Stress Analysis, (2020).
- [7] Šedková L., Vích, O. Temperature and damage-affected Lamb wave signals in a composite sandwich plate. Proceedings of the European Workshop on Structural Health Monitoring, (2022).
- [8] Mustapha, S., Ye, L., Dong, X., Alamdari, M. M. Evaluation of barely visible indentation damage (BVID) in CF/EP sandwich composites using guided wave signals. *Mech. Syst. Signal Process* (2016) **7677**:497–517.
- [9] Rose, J. L. *Ultrasonic Guided Waves in Solid Media*. Cambridge University Press, (2014).
- [10] Hettler, J., Tabatabateipour, M., Delrue, S., Abeele, K.V.D. Application of a Probabilistic Algorithm for Ultrasonic Guided Wave Imaging of Carbon Composites. *Phys. Procedia* (2015) **70**:664–667.
- [11] Wu, Z., Liu, K., Wang, Y., Zheng, Y. Validation and evaluation of damage identification using probability-based diagnostic imaging on a stiffened composite panel. *J. Intell. Mater. Syst. Struct* (2014) **26**:2181–2195.
- [12] Šedková, L. Structural health monitoring of aerospace composite structures using ultrasonic guided waves. (2022)
- [13] Bocchini, P., Marzani, A., Viola, E. Graphical User Interface for Guided Acoustic Waves. *J. Comput. Civ.* (2011) **25**:202–210.